Brain, Behavior, and Immunity 26 (2012) 919–930

Contents lists available at SciVerse ScienceDirect

Brain, Behavior, and Immunity

journal homepage: www.elsevier.com/locate/ybrbi

Prolongation of prion disease-associated symptomatic phase relates to CD3$^+$ T cell recruitment into the CNS in murine scrapie-infected mice

Antoine Sacquin [a,1], Thomas Chaigneau [a], Valérie Defaweux [b], Micheline Adam [c], Benoit Schneider [d], Martine Bruley Rosset [a,*], Marc Eloit [c]

[a] UMR-S 938, Hôpital St-Antoine, Bât. R. Kourilsky, 184 rue du Fg St-Antoine, 75012 Paris, France
[b] Centre d'Immunologie, Faculté de médecine, Université de Liège, 3 avenue de l'hôpital, 4000 Liège 1, Belgium
[c] UMR1161 Virologie, INRA, ANSES, ENVA, 7 avenue du général de Gaulle, 94704 Maisons Alfort, France
[d] Université Paris Descartes, Sorbonne Paris Cité, INSERM UMR-S747, 45 rue des Saints-Pères, 75006 Paris, France

ARTICLE INFO

Article history:
Received 11 January 2012
Received in revised form 5 April 2012
Accepted 9 April 2012
Available online 13 April 2012

Keywords:
Experimental prion disease
Prion protein
CD8$^+$ T cells
CNS infiltration
Vaccine
Adenovirus

ABSTRACT

Prion diseases are caused by the transconformation of the host cellular prion protein PrP^c into an infectious neurotoxic isoform called PrP^{Sc}. While vaccine-induced PrP-specific CD4$^+$ T cells and antibodies partially protect scrapie-infected mice from disease, the potential autoreactivity of CD8$^+$ cytotoxic T lymphocytes (CTLs) received little attention. Beneficial or pathogenic influence of PrP^c-specific CTL was evaluated by stimulating a CD8$^+$ T-cell-only response against PrP in scrapie-infected C57BL/6 mice. To circumvent immune tolerance to PrP, five PrP-derived nonamer peptides identified using prediction algorithms were anchored-optimized to improve binding affinity for H-2D^b and immunogenicity (NP-peptides). All of the NP-peptides elicited a significant number of IFNγ secreting CD8$^+$ T cells that better recognized the NP-peptides than the natives; three of them induced T cells that were lytic *in vivo* for NP-peptide-loaded target cells. Peptides 168 and 192 were naturally processed and presented by the 1C11 neuronal cell line. Minigenes encoding immunogenic NP-peptides inserted into adenovirus (rAds) vectors enhanced the specific CD8$^+$ T-cell responses. Immunization with rAd encoding 168NP before scrapie inoculation significantly prolonged the survival of infected mice. This effect was attributable to a significant lengthening of the symptomatic phase and was associated with enhanced CD3$^+$ T cell recruitment to the CNS. However, immunization with Ad168NP in scrapie-incubating mice induced IFNγ-secreting CD8$^+$ T cells that were not cytolytic *in vivo* and did not influence disease progression nor infiltrated the brain. In conclusion, the data suggest that vaccine-induced PrP-specific CD8$^+$ T cells interact with prions into the CNS during the clinical phase of the disease.

1. Introduction

Prion diseases are fatal transmissible neurodegenerative diseases in which a host-encoded protein, the cellular prion protein (PrP^c), is converted into an abnormally folded isoform called PrP^{Sc}. PrP^{Sc} is the main or only component of the infectious agent (Prusiner et al., 1998; Ma and Lindquist, 2002). These diseases are characterized by a long and asymptomatic peripheral incubation period followed by rapidly progressive and severe neurological dysfunctions and by specific pathological lesions of the CNS. To date, no cure has been found for prion diseases. Recently, immunotherapeutic approaches have been developed in experimental model of neurodegenerative diseases with some success (Peretz et al., 2001; White et al., 2003; Polymenidou et al., 2004; Schenk et al., 1999; Rosset et al., 2009). PrP antibodies inhibit the conversion of PrP^c to PrP^{Sc} *in vitro* (Beringue et al., 2004; Pankiewick et al., 2006) and confer some degree of protection against murine scrapie *in vivo* (Peretz et al., 2001; White et al., 2003; Polymenidou et al., 2004). Yet, they have been effective only during the peripheral lymphoreticular phase of the disease, presumably as a result of their poor blood–brain barrier penetration. Cell-mediated immunity against self-PrP^c has been less intensively explored as humoral immunity. Although PrPc is strongly expressed within the immune system (Bendheim et al., 1992), PrP-autoreactive CD4$^+$ T cells that have escaped thymic deletion

Abbreviations: PrP^c, cellular prion protein; PrP^{Sc}, prion protein scrapie; rAd, recombinant adenovirus; TSE, transmissible spongiform encephalopathy; AA, amino acid; Wt, wild-type; CTL, cytotoxic T lymphocytes; CNS, central nervous system; OligoCpG, oligodeoxy nucleotides; HBV, hepatitis B virus; *pi*, post-infection.

* Corresponding author. Tel.: +33 149 284 621; fax: +33 143 401 748.
E-mail address: martine.rosset@inserm.fr (M. Bruley Rosset).
[1] Present address: INSERM 1043, CHU Purpan, BP3028, 31024 Toulouse Cedex 3, France.

0889-1591/$ - see front matter © 2012 Elsevier Inc. All rights reserved.
http://dx.doi.org/10.1016/j.bbi.2012.04.002

were found in the blood of healthy donors (Isaacs et al., 2006). A variety of MHC-class II-restricted epitopes derived from human and murine PrP^c stimulated specific $CD4^+$ T cell responses when strong immunizing strategies were used (Gregoire et al., 2004; Rosset et al., 2004; Souan et al., 2001). $CD4^+$ T cell response against two PrP peptides in complete Freund's adjuvant led to a reduction in PrP^{Sc} level in prion-infected N2a tumor grafts (Souan et al., 2001). Adoptive transfer of $CD4^+$ T cells specific for $PrP_{156-170}$ peptide was able to attenuate prion disease in scrapie-infected mice (Gourdain et al., 2009). The efficiency of $CD4^+$ T cells was recently confirmed by the partial protection against the disease obtained after the transfer of transgenic T cells bearing a T cell receptor specific for PrP in the complete absence of PrP-specific antibodies (Iken et al., 2011). In these murine models, $CD4^+$ T cells seemed to contribute to prion-disease protection and not to cause harmful reactions in the CNS that expresses high levels of PrP^c and accumulates PrP^{Sc} when infected. T cells were shown to provide neuroprotection in chronic neurodegenerative diseases such as Amyotrophic Lateral Sclerosis (ALS) (Beers et al., 2011) and experimental Alzheimer's disease (AD) (Ethell et al., 2006). However, CNS-specific autoreactive $CD4^+$ T cells were described to be harmful in other models of neurodegenerative processes such as Parkinson's disease (Brochard et al., 2009), Experimental Autoimmune Encephalitis (EAE), Multiple Sclerosis (MS) (Mc Farland and Martin, 2007) and AD (Gilman et al., 2005). Moreover, meningoencephalitis that developed in a small proportion of AD patients during anti-Aβ AN1792 vaccination trial was attributed to pro-inflammatory T cell responses and associated with $CD4^+$ and $CD8^+$ T cells infiltrating the brain (Ferrer et al., 2004). Thus, in different neurodegenerative contexts, distinct T cell-type responses could positively or negatively influence disease progression.

While neuroprotection appears to be associated with CNS-infiltrating $CD4^+$ cells, the influence of potentially stimulated autoreactive $CD8^+$ has received little attention presumably because they are expected to be implicated in the direct killing of CNS cells and thus may induce brain lesions (Neumann et al., 2002). A role for $CD8^+$ T cells in autoimmune CNS demyelinisation was demonstrated by the development of EAE after transfer of MOG or MBP-specific $CD8^+$ T cells. In MS, the axonal damage intensity correlates with the number of $CD8^+$ T cells and macrophages in the lesions (Mars et al., 2007). Myelin-specific $CD8^+$ T cells closely interact with demyelinated axons in acute MS lesions and induce lysis of HLA-matched oligodendrocytes. With respect to prion diseases, the repertoire of $CD8^+$ T cells specific for PrP was poorly explored (Fernandez-Borges et al., 2006; Kaiser-Schulz et al., 2007). In Chandler-scrapie-infected non-immunized mice, $CD8^+$ cells specific for PrP-derived epitopes were detected in the spleen by tetramer staining but were not functional; in those infected mice, both $CD8^+$ and $CD4^+$ T cells infiltrated the brain without damaging neurons (Lewicki et al., 2003). Eight weeks after intracerebral injection with ME7, another murine scrapie strain, there was clear evidence of microglial activation and T cell recruitment in the brain and $CD8^+$ outnumbered $CD4^+$ cells. However, disrupting immune tolerance against PrP^c upon a vigorous stimulation can induce self-reactive $CD8^+$ T cells that can be deleterious in the CNS. In the case of prion diseases, CTLs specific for self-PrP might be unable to discriminate between healthy and infected cells as PrP^c and PrP^{Sc} share the same amino acid (AA) sequence. Conceivably, the accumulation of PrP^{Sc} in prion-infected cells will result in greater presentation of PrP-derived epitopes, enabling CTLs specific for PrP^c to preferentially target PrP^{Sc}-laden infected cells as frequently observed for CTLs recognizing over expressed tumor self-antigens (Gross et al., 2004).

The goals of this work were first to identify immunogenic PrP-derived H-$2D^b$-restricted peptides and to analyze the protective or pathogenic effect of $CD8^+$ CTLs targeting these epitopes on prion disease progression, and particularly in the CNS of scrapie-infected mice. For this purpose, we used immunization strategies eliciting PrP-specific $CD8^+$ T cells and avoiding concomitant development of humoral and $CD4^+$ T cells.

2. Materials and methods

2.1. Mice and ethics statement

C57BL/6 mice were purchased from Charles Rivers. PrP-deficient (*Prnp*$^{-/-}$) mice knock out for the murine *Prnp* gene were kindly gifted by Dr. C. Weissmann (Institute of neurology, London, UK) and they have been iteratively back-crossed in our animal housing facility with C57BL/6 progenitors. They were maintained under strict, specific pathogen-free conditions in accordance with good animal practice as defined by the relevant national and/or local animal welfare bodies, and all animal work was approved by the local ethics committee of the Alfort School of Veterinary Medicine.

2.2. Plasmids and peptides

A pcDNA3.1 vector containing the murine *PrP* sequence (mPrP) encoding the 23–232 protein was used for DNA vaccination as already described (Gregoire et al., 2004). Empty pcDNA3.1 plasmid was used as control. Nonamer peptide sequence bearing H-$2D^b$-binding motifs were selected by applying the epitope prediction algorithm BIMAS (www-bimas.cit.nih.gov/) to mPrP AA sequence. AAs were substituted at 1, 2, 3, 5 and 9 H-$2D^b$ anchor positions by AAs from a high binding-affinity peptide from the influenza nucleoprotein (NP366). These modified peptides were mentioned as NP-peptides. Native and modified peptides were synthesized (purity >90%) by Genecust (Evry, France). Plasmids p168NP, p217NP and pTA were introduced into adenovirus type 5 (Ad5) as indicated in Fig. 1. Synthetic genes optimized for expression in mice were constructed by Geneart (Regensburg, Germany), put under the control of the hCMV promoter, and inserted into an Ad5 vector as described previously (Branger et al., 2001). For controls, we used AdTA, an isogenic Ad5 expressing a non-relevant polypeptide.

2.3. Immunization protocols and prion challenge

For immunization, *Prnp*$^{-/-}$ mice received two or three intra-muscular (*im*) injections of 100 μg of PrP-pcDNA at weekly interval. These mice were sensitized 5 days before with 50μgl cardiotoxin. C57BL/6 mice were injected subcutaneously (*sc*) at the base of the tail with 100 μg of peptide, 50 μM of oligo-CpG (No. 3678), and 100 μg of the I-A^b-binding HBV core peptide emulsified

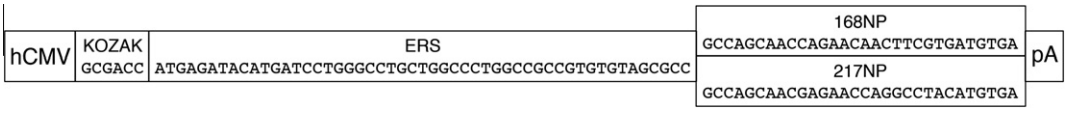

Fig. 1. Structure of the genes encoding CD8 peptides: a KOZAK sequence, followed by the human adenovirus 2 E3/19K endoplasmic reticulum translocation signal sequence (ERS) fused with the peptide sequence (168NP or 217NP), was inserted downstream of the hCMV promoter and upstream of the polyA sequence.

in an equal volume of incomplete Freund's adjuvant. Immunization was also performed by intramuscular (*im*) injection of rAds at a dose of 10^8 TCID50. Three weeks later, each animal received a booster *im* injection of 50 μg of the corresponding plasmid vector. Control mice received AdTA or pTA. The mice were challenged intraperitoneally (*ip*) with 100 μL of 0.5% brain homogenate from terminally ill 139A-infected mice ($10^{4.33}$ LD50). Figures illustrate the immunization protocol for each assay. Disease progression was monitored by observing the mice twice a week from 20 weeks post-infection (*pi*) onward. Activity levels and competence were assessed on a set of parallel bars as described previously (Levavasseur et al., 2007).

2.4. Measurement of relative affinity of peptides for H-2D^b

RMAS lymphoma cells were incubated for 4 h at 27 °C with various concentrations of peptides. Cells were then washed and cultured for an additional 4 h period at 37 °C in complete culture medium without peptides. For staining, 2×10^5 RMAS cells were incubated for 20 min at 4 °C with biotin-conjugated H2-D^b-specific monoclonal antibody (mAb) (clone 28-14-8, BD Biosciences), followed by phycoerythrin-conjugated streptavidin. Samples were analyzed on a FACS Calibur flow cytometer using Cell Quest software (Becton–Dickinson). Cell-surface fluorescence is expressed as mean fluorescence intensity (MFI).

2.5. Indirect immunofluorescence on EL4 cells for anti-native PrP^c antibody testing

Antibody binding to cell-surface native PrP^c was detected by immunofluorescence staining using the EL4 T cell line as described (Gregoire et al., 2004). Since EL4 cells express low level of PrP^c, they were stably transfected with the *Prnp* gene and activated with anti-CD3mAb (clone 2C11) before each test to enhance PrP expression. The specificity of this assay for detecting anti-native PrP^c antibodies was previously validated on non-transfected EL4 cells. The level mPrP expression on EL4 cells after activation was checked using anti-PrP mAb (SAF83 mAb given by Dr. Grassi, CEA, France). EL4 cells were incubated with control or immune sera diluted 1/10 for 20 min at 4 °C, washed and revealed by adding PE-labeled rat anti-mouse IgK mAb for 20 min. Every assay included anti-mouse IgK mAb alone as back-ground control and SAF83 mAb as the upper limit. Samples were analyzed on a FACS Calibur flow cytometer using Cell Quest software (Becton–Dickinson). Cell-surface fluorescence is expressed as mean fluorescence intensity (MFI).

2.6. ELISPOT assay

Nitrocellulose-based 96-well plates (Millipore) were coated with anti-mouse IFN-γ capture mAb (1/500) (BD Biosciences) and saturated with complete culture medium. Responder splenocytes from individual mice were seeded at a dose of 10^6 or 5×10^5 cells/wells and stimulated with medium or 10 μg/ml of peptide. In some experiments, splenocytes were stimulated with mitomycin-treated 1C11 cells (2×10^4/wells), a neuronal cell line. Purified CD8$^+$ splenocytes were isolated using Dynal mouse CD8 negative isolation kit (Invitrogen Dynal). Bone marrow-derived dendritic cells were used as APCs (2×10^4/wells) in the case of purified CD8$^+$ responder cells (10^5/wells). Plates were incubated at 37 °C in 5% CO_2 for 18 h, washed, and incubated with biotinylated anti-mouse IFNγ detection mAb (BD Biosciences). Then, alkaline phosphatase conjugated to streptavidin was added (Roche) (1/500 dilution, 100 μL/well). IFNγ-secreting cells were visualized using tetrazolium nitroblue/bromo chloro-indolylphosphate (TNB/BCIP) substrate (Promega) and spots were counted using an automatic ELISPOT plate reader (ICI). Test wells were assayed in triplicate and the frequency of peptide-specific T cells was calculated after subtracting the mean number of spots obtained in the absence of peptide. Spot frequencies lower than 20 were considered non-significant.

2.7. In vivo cytotoxicity assay

CTLs were detected based on the *in vivo* clearance of CFSE-stained target cells (Vybrant CFDA SE Cell Tracer Kit; Molecular Probes). Splenocytes from C57BL/6 and *Prnp*$^{-/-}$ mice were used as targets expressing or not PrP^c, respectively, to evaluate the CTLs induction following immunization of *Prnp*$^{-/-}$ mice with PrPpcDNA. Splenocytes from *Prnp*$^{-/-}$ mice were loaded with NP-peptides and stained with 5.0 μM CFSE (CFSE^{high}). Control splenocytes from *Prnp*$^{-/-}$ mice were loaded with a control peptide (366NP) and stained with 0.5 μM CFSE (CFSE^{low}). CFSE-labeled control and experimental splenocytes (10^7 each, mixed 1:1) were injected *iv* into immunized or naive mice. Splenocytes were collected 18 h later and analyzed by flow cytometry. The percentage of specific cytotoxicity was calculated using the formula:

$$\left[1 - \left(\frac{\frac{CFSE_{exp}^{high}}{CFSE_{exp}^{high}+CFSE_{exp}^{low}}}{\frac{CFSE_{ctl}^{high}}{CFSE_{ctl}^{high}+CFSE_{ctl}^{low}}}\right)\right] \times 100$$

where CFSE^{high} was the number of PrPc or peptide-specific targets and CFSE^{low} the number of control (either *Prnp*$^{-/-}$ or control peptide loaded) targets recovered from either naive (ctl) or immunized (exp) mice.

2.8. In vitro ^{51}Cr release cytotoxic assay

Spleen cells from immunized mice were cultured at 37 °C with the corresponding NP-peptide in complete medium. RMAS or 1C11 target cells were labeled with ^{51}Cr for 1 h at 37 °C and incubated (10^4 cells/wells) with 10 μg/mL of native or NP-peptides for 2 h in 96-well round-bottom plates. Various concentrations of effectors were added in triplicate, and culture supernatants were collected 4 h later. ^{51}Cr release (cpm) was measured in a γ counter (LKB). The percentage of cytotoxicity was estimated as follows: [1 − (experimental release − minimum release/maximum release − minimum release) × 100], where minimum was the amount of ^{51}Cr released by peptide/RMAS-labeled cells without effectors and maximum the total amount of ^{51}Cr obtained after lysis of 10^4 RMAS or 1C11 cells.

2.9. Monitoring the percentage of peptide-specific CD8$^+$ T cells in immunized mice

Blood was collected at different time points after vaccination as indicated in the text and red blood cells were lysed. The frequency of 217NP- and 192NP-specific CD8$^+$T cells was estimated by labeling with biotin-conjugated NP-peptide/H-2D^b pentamers (Proimmune). The frequency of peptide-specific CD8$^+$ cells was also assessed by intracellular IFN-γ staining of CD8$^+$ cells after 4 h of incubation with the native and NP-peptides (Cytofix/Cytoperm Plus Golgi Plug Kit, BD Biosciences). The percentage of IFN-γ$^+$CD8$^+$ was evaluated by FACS.

2.10. Histological and immunohistochemical procedures

CD3$^+$ immunolabeling: brains collected at the terminal stage of the disease were fixed in PBS containing 10% paraformaldehyde (Merck) and embedded in paraffin. Sections of 5 μm performed on a Leica RM2145 microtome were mounted on Superfrost glass slides (Unimark, Marienfeld), deparaffinised and hydrated. As

antigen retrieval procedure, the samples were submitted during 20 min to 120 W microwaves immersed in citrate buffer containing 0,05% Tween-20 at pH 6.6 and then cooled at room temperature for 30 min. Immunolabeling was performed using anti-CD3 mAb (diluted 1/200, clone SP7, Spring Bioscience) revealed with an Alexa Fluor 488-conjugated goat anti-rabbit secondary antibody (Invitrogen). CD3/CD4/CD8 immunolabeling: brains were frozen in OCT compound (Tissue-Tek Sakura) and 5 μm-cryosections were labeled with rabbit anti-mouse $CD3^+$ mAb (revealed with an Alexa Fluor 488-conjugated goat anti-rabbit) in combination with rat anti-mouse $CD4^+$ or $CD8^+$ mAbs (Relia Tech Gmb) revealed with Alexa Fluor 594-conjugated goat anti-rat mAb. At least three non-adjacent sections in the forebrains, midbrains and hindbrains were analyzed and Dapi-stained positive cells were counted. Numbers were normalized for the tissue section surface area calculated by the Image J software. Three mice per treatment were examined and the numbers of $CD3^+$-, $CD4^+$-, and $CD8^+$-positive cells per mm^2 were compared using Student's *t* test.

2.11. Statistical analyses

Analyses were performed with GraphPad software and values were considered as significantly different for $P < 0.05$. Clinical phase duration was presented using Kaplan Meier survival curves. The Logrank Test was used for comparison between survival curves. Mean precursor frequencies were compared using Student's *t* test.

3. Results

3.1. Generation of anti-PrP cytotoxic T lymphocytes (CTLs)

We previous reported that immunization of $Prnp^{-/-}$ mice with mPrP encoding plasmid (PrP-pcDNA) elicits the generation of $CD4^+$ T cells specific for class II-restricted PrP peptides and the production of antibodies directed against native PrPc (Gregoire et al., 2004). The same approach was used here to identify immunogenic epitopes able to stimulate CTLs against PrP. Five $Prnp^{-/-}$ mice were immunized with 100 μg of PrP-pcDNA and four received the empty plasmid as control at weekly interval. PrP-specific lytic activity was evaluated 10 days after the second or the third immunization set by injecting mice with a mixture of $Prnp^{-/-}$ and of $CFSE^{high}$ C57BL/6 splenocytes. Their spleens were analyzed by flow cytometry 18 h after *in vivo* cell injection. Fig. 2A represents a typical overlay showing the number of $CFSE^{low}$ $Prnp^{-/-}$ and $CFSE^{high}$ C57BL/6 cells remaining in the spleen. No difference in the number of C57BL/6 was detected in PrP-immune mice versus control mice indicating a lack of cytotoxicity. Sera were collected after the second and third immunizations and the presence of antibodies specific for native PrPc was measured through their capacity to bind to the surface of PrP-transfected EL4 cells previously activated by anti-CD3 mAb. Fig. 2B illustrates one example of serum antibody binding to EL4 cells, the PrPc expression level is measured by the fluorescence intensity obtained after binding of SAF83 mAb-specific for PrPc. The percentage of *in vivo* lysis of $CFSE^{high}$-labeled targets, calculated as described in Materials and Methods, and the level of antibodies expressed as mean intensity fluorescence (MFI) are shown in Fig. 2C. Three mice were killed after two PrP-pcDNA injections and two mice after three injections. Two empty plasmid treated-mice served as controls. The results indicated that no PrP-specific cytotoxicity occurred in PrP-immune mice whether they received two or three PrP-pcDNA immunizations (Fig. 2C). In contrast, the detection of anti-PrPc antibodies in all PrP-cDNA immune sera which levels increased after the third

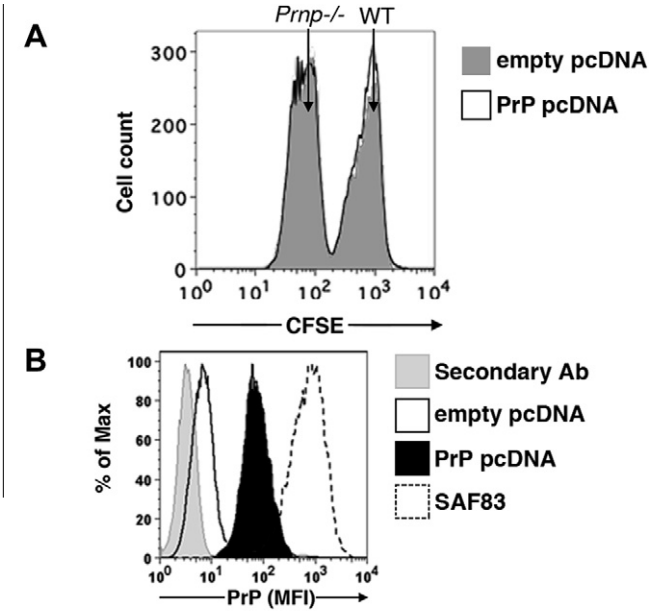

C

Immunization of *Prnp-/-* mice with	mice number	% *in vivo* lysis of CFSE-labeled targets		Level of serum antibodies (MFI)	
		Two immunizations#	Three immunizations#	Two immunizations#	Three immunizations#
PrP pcDNA	1	1,35	NT	112	NT
	2	0	NT	48	NT
	3	6,95	NT	59	NT
	4	NT	5,5	103	212
	5	NT	0	70	230
Empty pcDNA	1	0	NT	20,7	NT
	2	0	NT	21,6	NT
	3	NT	0	NT	21,6
	4	NT	0	NT	20,8

#In vivo cytotoxicity test and serum collection were performed 10 days after the last immunization

Fig. 2. Effect of DNA vaccination on the development of immune responses in $Prnp^{-/-}$ mice. pcDNA3.1 vector encoding or not PrP^c was injected *im* two or three times at weekly interval at a dose of 100 μg/mouse. (A) *In vivo* PrP-specific lytic activity was evaluated 10 days after the last immunization by inoculating a mixture of $CFSE^{low}$ $Prnp^{-/-}$ and $CFSE^{high}$ C57BL/6 splenocytes into empty pcDNA- or PrP-pcDNA-immunized $Prnp^{-/-}$ mice. Splenocytes from recipient mice were collected 18 h after injection and analyzed by flow cytometry. A typical overlay showing the number of $CFSE^{low}$ $Prnp^{-/-}$ and $CFSE^{high}$ C57BL/6 cells remaining in the spleens of one empty pcDNA (gray histogram) and one PrP-pcDNA (empty histogram)-immunized $Prnp^{-/-}$ mice is presented. (B) Sera were collected 10 days after the last immunization and antibody response was measured by incubating the sera from empty pcDNA- or from PrP-pcDNA-immunized $Prnp^{-/-}$ mice with PrP^c-transfected EL4 cells using indirect immunofluorescence. Their binding was revealed by adding PE-labeled anti-mouse IgK. Typical overlay of EL4 cells incubated with the secondary antibody alone and with an empty pcDNA- or a PrP-pcDNA-immunized serum. Secondary antibody alone served as negative control and anti-PrP mAb (SAF 83) served as upper limit. (C) Quantitative results of cytotoxicity and antibody level after DNA immunization: the percentage of *in vivo* specific lysis of CFSE-labeled cells was calculated as described in Materials and Methods. Anti-PrP antibody level is expressed as mean fluorescence intensity (MFI) of EL4 cells incubated with a 1/10-diluted serum. Each value represents one individual mice.

immunization step, signed the efficacy of the immunization procedure. Hence, while this immunizing regimen was able to induce humoral response, it did not stimulate PrP-specific CTLs.

We thus analyzed mPrP for nonamer peptide sequences bearing $H\text{-}2D^b$ binding motifs by using the epitope prediction algorithm BIMAS (Fig. 3A, left panel). The affinity of five synthetic candidate peptides was measured through their capacity to bind and stabilize the $H\text{-}2D^b$ molecules at the surface of RMAS cells. These cells are deficient for TAP molecules in charge of endogenous peptide transport, and thus express empty and unstable class I molecules. The

expression level of class I was detected by a PE-conjugated H-2D^b specific mAb (MFI) at the surface of RMAS cells. Incubation with 10 μg/mL of five candidate peptides induced only low class I expression when compared to incubation with a high affinity peptide (NP366) (Fig. 3B, left panel).

Wt mice were immunized with these peptides in combination with an I-A^b-restricted CD4$^+$ helper epitope (HBV core) and CpG/IFA. No immune response specific for the class I-restricted PrP-derived peptides were detected in the spleen of immunized mice while a significant number of splenocytes secreted IFNγ in response to HBV (Fig. 3C, left panel). The same immunizing regimen applied to *Prnp*$^{-/-}$ mice also induced weak T cell responses (Supplemental 1), indicating that the lack of immune responses in wt mice relates to the low binding affinity of native peptides. AA substitutions were introduced at MHC class-I anchor positions of the different peptides (Fig. 3A, right panel). Binding affinities for H-2D^b were largely improved for all NP-modified peptides (Fig. 3B, right panel) and four of them elicited a significant number of IFNγ-secreting splenocytes. Of note, the recruited repertoires consistently responded to NP-peptides better than to the corresponding native peptides (Fig. 3C, right panel).

Cytotoxicity was evaluated in NP-peptide-immunized wt mice based on the *in vivo* clearance of CFSE-labeled target cells. No traces of specific lysis could be evidenced against target cells loaded with native peptides, likely due to the rapid *in vivo* dissociation of peptide/H-2D^b complexes (Table 1). In contrast, we found substantial specific lysis of NP-peptide-loaded target cells *in vivo* in mice immunized with 168NP, 192NP, or 217NP. The *in vitro* ^{51}Cr release assay showed that only 217NP-induced T cells were cytotoxic toward RMAS cells loaded with either native or NP-peptides (Table 1). These results indicate that the immunizing peptides must be modified to ensure CTL recruitment. To determine if these peptides are naturally processed by cells expressing PrP, we used the mPrP-expressing 1C11 neuronal cell line (Buc-Caron et al., 1990; Mouillet-Richard et al., 2000), which express H-2D^b class I but not I-A^b class II molecules at the cell surface (data not shown). Wt mice were immunized with 168NP, 192NP, and 217NP mixed in HBV/CpG/IFA as described above. Fig. 4 indicates that the three peptides induced a sizeable CD8$^+$ T cell population secreting IFNγ in response to the corresponding NP peptides. Total splenocytes and CD8$^+$-purified T cells from mice immunized with 168NP and 192NP but not with 217NP secreted IFNγ in response to exposure

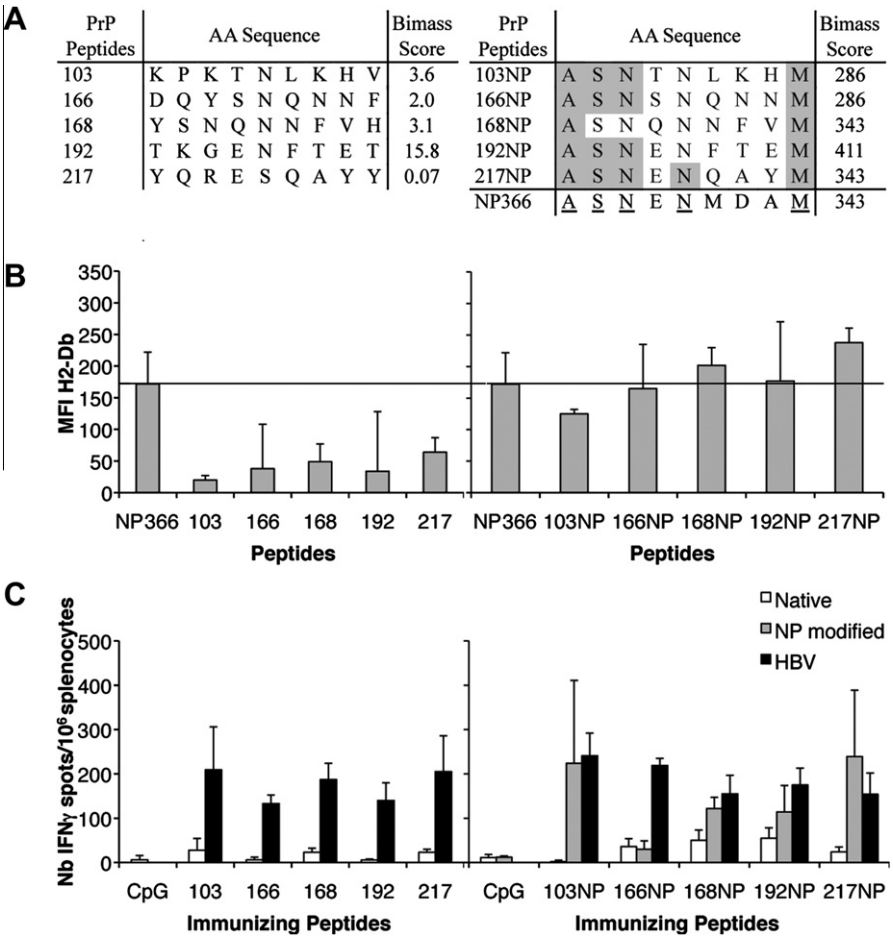

Fig. 3. Sequence, binding affinity and immunogenicity of PrP peptides. (A) AA sequence of nonamer peptides derived from PrP using the BIMAS prediction algorithm (left panel). PrP peptides were modified by replacing AAs at the H-2Db anchor sites by AAs from a high binding-affinity peptide, the influenza virus nucleoprotein (NP366) to produce NP-peptides (right panel). (B) RMAS cells were incubated for 4 h with 10 μg/ml of peptides and cell surface MHC class I expression was evaluated after staining with anti-H-2D^b mAb. Binding affinity is reported as mean MFI ± SD of several experiments (n) for each native peptide (left panel: 103, n = 2; 166, n = 3; 168, n = 3; 192; n = 5, 217, n = 2) or NP-peptide (right panel: 103NP, n = 6; 166NP, n = 5; 168NP, n = 5; 192NP, n = 5; 217NP, n = 4). NP366 served as a high-affinity reference peptide (n = 5). (C) Frequency of IFN-γ-secreting splenocytes in peptide-immunized wt mice, as assessed by ELISPOT. Spleen cells (10^6/wells) from mice immunized with native (left panel) or NP-peptides (right panel) in CpG/HBV/IFA or with PBS/CpG/HBV/IFA alone were stimulated in triplicate for 18 h at 37 °C with the corresponding peptide in a concentration of 10 μg/ml. The results are reported as the mean numbers of peptide-specific IFN-γ-secreting T cells ± SD per 10^6 spleen cells from 2 to 4 mice calculated after subtracting the mean number of spots obtained in the absence of peptide. n = number of immunized mice for each native peptide (left panel: CpG, n = 4; 103, n = 2; 166, n = 2; 168, n = 4; 192; n = 3, 217, n = 3) or NP-peptide (right panel: CpG, n = 7; 103NP, n = 2; 166NP, n = 2; 168NP, n = 4; 192NP, n = 7; 217NP, n = 7).

Table 1
Capacity of wt mice immunized with NP-peptides to lyse *in vivo* and *in vitro* target cells loaded with native or NP-peptides.

% *in vivo* lysis of CFSE-labeled target loaded with peptide (mean ± SD)			% *in vitro* cytotoxicity for 51Cr labeled RMAS loaded with peptide (mean ± SD)						
Immunizing peptide	Native peptide	NP-peptide	Immunizing peptide	Native peptide			NP-peptide		
			E:T ratio:	50/1	25/1	12/1	50/1	25/1	12/1
CpG ($n = 2$)	0.6 ± 0.2	0.5 ± 0.5 ($n = 3$)[a]	CpG ($n = 7$)[a]	11.5 ± 7.7	8.9 ± 5.3	3.3 ± 1.7	10.1 ± 8.1	6.6 ± 5.0	2.7 ± 2.6
168NP	1.3 ± 0.2 ($n = 2$)	41 ± 7 ($n = 2$)	168NP ($n = 4$)	8.9 ± 5.1	5.3 ± 2.6	2 ± 1.3	10.9 ± 4.1	6 ± 2.3	3.1 ± 1.6
192NP	NT	48 ± 10 ($n = 6$)	192NP ($n = 4$)	9.4 ± 6.6	7.4 ± 4.7	4.4 ± 4.2	10.9 ± 8.9	6.3 ± 5.0	3.1 ± 1.6
217NP	1.7 ± 0.4 ($n = 2$)	94 ± 2 ($n = 4$)	217NP ($n = 4$)	40.5* ± 12.3	31.8* ± 12.8	19.7* ± 9.2	39.7* ± 17.3	33* ± 18	13.8 ± 13

[a] Number of mice per group.
* Significantly different compare to CpG control value ($p < 0.05$) by Student's t test.

to mitomycin-treated 1C11 cells (Fig. 4). This suggests that 168 and 192 but not 217 are naturally processed epitopes of PrP. The specificity of the immune splenocytes for the NP-peptides was shown by the absence or the low reactivity toward 366NP which is specific for the nucleoprotein of influenza virus but possesses AA at H-2Db anchor position identical to all NP-modified peptides. However, immunized splenocytes failed to lyse 1C11 cells in an *in vitro* ^{51}Cr release assay (data not shown).

3.2. Effect of NP-peptide immunization in scrapie-infected mice

Wt mice were immunized twice with any of the three NP-peptides in the presence of HBV/CpG/IFA, and then inoculated 10 days later with 0.5% 139A brain homogenate from terminally ill scrapie mice. Ten weeks post-infection (*pi*), IFN γ-secreting T cells specific for the immunizing NP-peptides were observed in the spleen as determined by ELISPOT. Disease progression was monitored by assessing activity levels and competence from 20 weeks post-infection onward (Levavasseur et al., 2007). In these experimental conditions, no significant modification in the disease progression

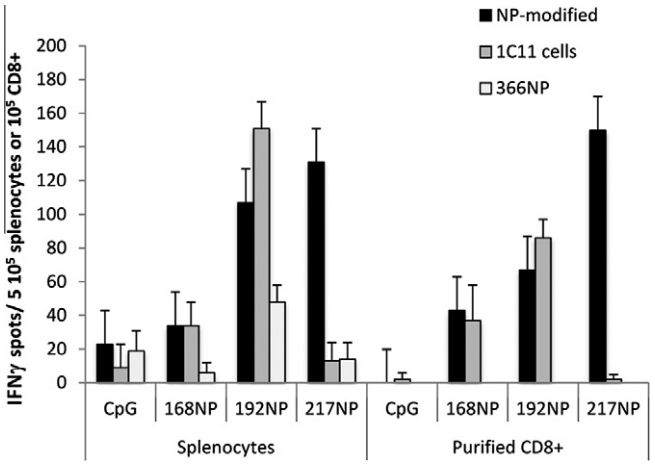

Fig. 4. Frequency of peptide-specific CD8$^+$ T cells in PrP-peptide immunized wt mice. Mice were immunized with 168NP, 192NP, or 217NP in CpG/HBV/IFA or with PBS in CpG/HBV/IFA alone. Spleen cells (5 10^5/well) were stimulated for 18 h at 37 °C with 10 μg/ml of NP-peptides, 366NP control peptide or with mitomycin-treated 1C11 cells (2×10^4/wells). 1C11 cells express H-2D^b class I but not Ia^b class II molecules. Results are presented as the mean numbers of peptide-specific IFN-γ secreting cells ± SD per 5×10^5 spleen cells from 2 to 4 mice (left panel). CD8$^+$ cells were purified from pooled immunized splenocytes using a negative selection kit (Dynal). CD8$^+$ cells (10^5 cells/wells) were stimulated either by DC-loaded NP peptides or with mitomycin-treated 1C11 cells (2×10^4/wells). Results are reported as numbers of peptide-specific IFN-γ-secreting CD8$^+$ T cells per 10^5 cells calculated after subtracting the number of spots obtained in the absence of peptide or cells.

was observed between peptide-treated and untreated 139A-infected mice (Supplemental 2).

To increase the size of the specific CD8$^+$ repertoire, minigenes encoding immunogenic NP-peptides were inserted into adenovirus (rAds) and used as immunogens. These vectors improve antigenic presentation and bring strong helper signals. Two peptides were selected: 168NP which stimulates a cytolytic repertoire reacting with a naturally processed epitope and 217NP for which the corresponding CD8$^+$ specific repertoire only recognized peptide-loaded targets but not PrP-expressing cells. A control rAd (AdTA) was used to evaluate the contribution of Ad antigens alone. Wt mice were immunized with rAds followed three weeks later by a booster immunization with the corresponding plasmids (p168NP, p217NP, and pTA) (Fig. 5A, Exp. 1). The day before 139A-infection, CD8$^+$ T-cell responses were quantified in the blood of rAd-immunized mice by peptide-specific pentamer-binding or intracellular IFNγ production. The percentage of 217NP/H-2D^b pentamer-binding CD8$^+$ cells was 1.87 ± 0.49% ($n = 8$; $p = 0.05$ compared to AdTA; Fig. 5B, left panel). The percentage of CD8$^+$ cells producing intracellular IFNγ in response to 168NP was 0.96 ± 0.24% ($n = 7$; $p = 0.044$ compared to AdTA; Fig. 5B, right panel). Nine weeks *pi*, the peptide-specific CD8$^+$ T cell population was either expanded or unchanged. Two mice per group were then sacrificed and the frequency of IFNγ-secreting splenocytes was quantified by ELISPOT in response to NP-modified peptides and their native counterparts. Specific T cells better recognized 217NP than native 217 peptide while in Ad168NP immunized mice, responses to native and modified peptide were nearly similar (Fig. 5C). In addition, the cytotoxic capacity of two immunized mice per group was evaluated by the *in vivo* clearance of CFSE-labeled NP-peptide-loaded targets (Table 2). Percentage of *in vivo* lysis was higher in mice given Ad168NP (92%) than in mice given Ad217NP (72%) and contrasted with results obtained after peptide immunization (41% for 168NP versus 94% for 217NP; Table 1) indicating the potency of Ad constructs to stimulate CTLs. The prion disease natural history includes a long and asymptomatic incubation period (time from 139A inoculation to symptoms onset) and a clinical phase (time from symptoms onset to death). The survival times were not modified whatever the treatment received by scrapie-infected mice (Table 3, Exp. 1). Yet, the clinical phases but not the incubation periods were slightly ($p = 0.028$) prolonged after Ad168NP immunization when compared to untreated infected but not to AdTA-treated mice (Fig. 5C).

3.3. Expansion of the 168-specific CD8$^+$ T cell repertoire improved protection against murine scrapie

To further amplify and sustain the pool of specific CD8$^+$ T cells, mice primed/boosted with Ad168NP/plasmid received two additional injections of the native 168/CpG/IFA 4 weeks apart (Fig. 6A, Exp. 2). The mean percentage (±SD) of intracellular IFNγ-producing

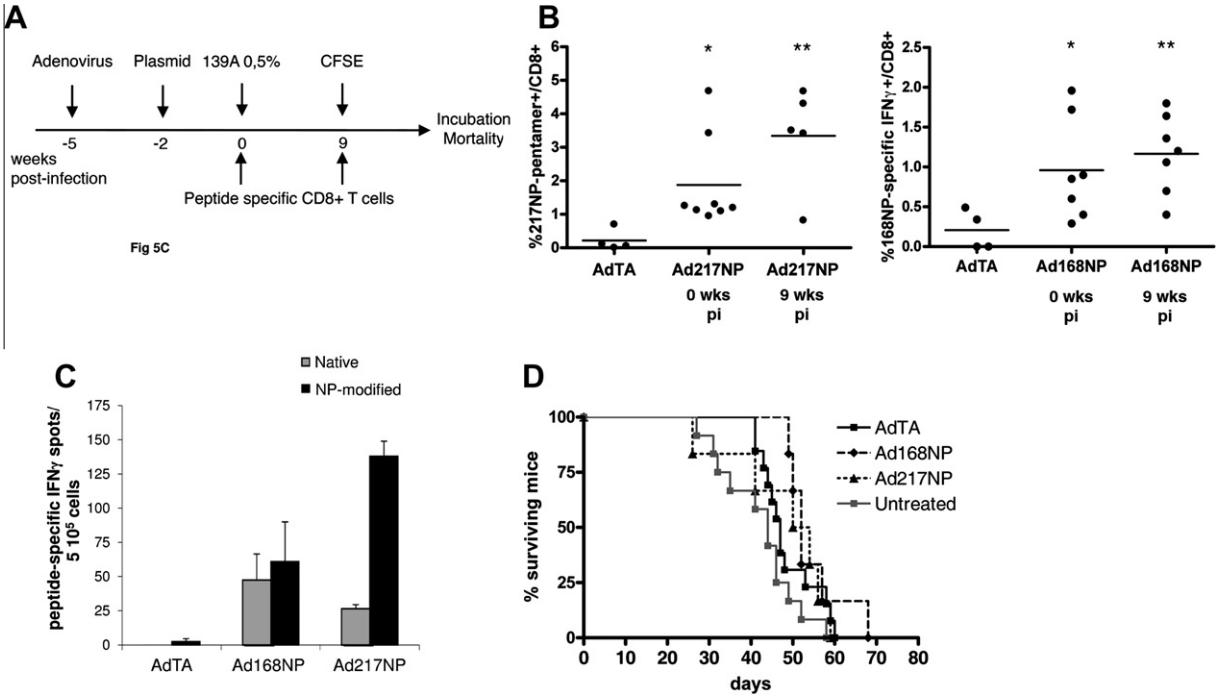

Fig. 5. Effect of prophylactic immunizations with Ad168NP, Ad217NP or AdTA on specific $CD8^+$ T-cell responses and murine scrapie. (A) Time-sequence of immunization, plasmid boost and scrapie injection in C57Bl/6 mice. Wt mice were immunized with AdTA ($n = 16$), Ad217NP ($n = 10$), or Ad168NP ($n = 10$) then received a plasmid boost and two weeks later an injection of 139A scrapie. (B) Frequency in the blood of rAd-immunized mice of $CD8^+$ cells binding to 217NP/H-$2D^b$ pentamers or producing intracellular IFN-γ after 4 h activation with 168NP peptide at different time points *pi* (upper panel). Significance: $^*p \leqslant 0.05$; $^{**}p < 0.01$. (C) Frequency by ELISPOT of IFN-γ-secreting splenocytes from two Ad-immunized mice nine weeks *pi* (lower panel). Spleen cells (5×10^5/wells) from immunized mice were stimulated in triplicate for 18 h at 37 °C with the native or NP-peptide at 10 μg/ml. The results are presented as the mean number of peptide-specific IFNγ-secreting cells per 5×10^5 spleen cells ± SD from two mice calculated after subtracting the mean number of spots obtained in absence of peptide. (D) Mice were weekly examined for early signs of disease beginning at 5 months *pi* in each of the immunized groups. Mortality was recorded and Kaplan Meir survival curves was used to show the clinical stage duration which represents the time (days) elapsing from the beginning of the clinical symptoms to the death.

Table 2
Lytic capacity of Ad-immunized mice infected with 139A.

Immunization of 139A infected mice	% *in vivo* specific lysis of CFSE-labeled *Prnp*$^{-/-}$ splenocytes loaded with NP-peptides
AdTA	1 ± 1
Ad168NP	92.5 ± 7.8
Ad217NP	72 ± 5.6

Each value corresponds to the mean of two mice ± SD.

$CD8^+$ cells in the blood 5 weeks *pi* was low in response to the native 168 peptide (0.05 ± 0.01%; $n = 8$; Fig. 6B) but significantly increased in response to 168NP (0.85 ± 0.06%; $p < 0.0001$) as compared to AdTA-treated mice (0.16 ± 0.05%; $n = 6$; Fig. 6C). Interestingly, the boost with 168 induced a significant reactivity of $CD8^+$ T cells for native peptide (0.29 ± 0.08%; $p < 0.03$). These $CD8^+$ T cells were specific for the 168 peptide since stimulation with 366NP control peptide failed to induce any IFNγ production (data not shown). Survival time was significantly increased in AdTA ($p = 0.0005$) and in Ad168NP-treated mice ($p = 0.0002$) when compared to untreated 139A-infected mice (Table 3, Exp. 2). This effect was not due to a prolongation in the asymptomatic incubation phase but to a significant lengthening in the clinical phase duration observed in AdTA ($p = 0.0044$) and in Ad168NP-treated mice ($p = 0.0003$) when compared to untreated 139A-infected mice (Fig. 6E). In this experiment, Ad168NP treatment further enhanced ($p = 0.052$) the clinical phase duration compared to AdTA-treated mice (Table 3, Exp. 2) suggesting a peptide-specific effect.

T cell infiltration was quantified in three nonadjacent sections of paraffin-embedded brains of three terminally ill mice for each treatment, using indirect immunofluorescent staining with anti-CD3 mAb. Data depicted in Fig. 6D indicated that T cells were nearly undetectable in the midbrain region of CNS of non-infected wt mice ($m = 0.014 \pm 0.006/mm^2$), and their number increased eight fold following 139A infection ($m = 0.112 \pm 0.024/mm^2$; $p < 0.001$). $CD3^+$ cells further accumulated after AdTA ($m = 0.384 \pm 0.07/mm^2$; $p = 0.054$) and Ad168NP treatment ($m = 0.582 \pm 0.07/mm^2$; $p = 0.006$) when compared to untreated 139A-infected mice. Although the difference between Ad168NP and AdTA-treated did not reach statistical significance, a trend ($p = 0.07$) is observed toward an increased number of $CD3^+$ T cells in the brain of Ad168NP-treated mice. Similar results were observed after rAd treatments in the forebrains and hindbrains regions (data not shown). $CD4^+$ and $CD8^+$ characterization of the $CD3^+$ population failed because of the absence of mAbs working with paraffin-embedded sections. T cells infiltrated the parenchyma in the striatum, thalamus, hypothalamus and hippocampus, and were found in abundance in the cerebral cortex surrounding zones of typical spongiosis.

3.4. Therapeutic immunization with 168NP-encoding rAd/plasmid failed to protect scrapie-infected mice

As Ad168NP immunization extended the symptomatic phase when performed before scrapie inoculation, we evaluated its effect in scrapie-incubating mice (10 weeks *pi*) when secondary lymphoid organs are fully invaded by prions (Fig. 7A; Exp. 3). The mean percentage (±SD) of intracellular IFNγ-producing $CD8^+$ T cells in the blood was significantly increased in response to 168NP (0.45 ± 0.08%; $n = 10$; $p < 0.0001$; Fig. 7B) following Ad/plasmid prime/boost (15 weeks pi) and remained constant through the period of observation (0.42 ± 0.08%; $n = 10$; $p < 0.0001$ at 17 weeks pi and 0.47% ± 0.08; $p < 0.0001$ at 19 weeks pi). Yet, $CD8^+$ T cell

Table 3
Effects of the various immunization regimens on incubation time, clinical phase and survival time in WT mice inoculated with 139A scrapie.

			Incubation Phase		Clinical Phase		Survival Time	
		Nb of mice	Mean days ± SD	p^a	Mean days ± SD	p^a	Mean days ± SD	p^a
Exp. 1: rAd/Plasmid immunization	Untreated	12	169 ± 3		42 ± 9		212 ± 9	
	AdTA	12	175 ± 10	ns	49 ± 7	ns	221 ± 13	ns
	Ad168NP	6	168 ± 6	ns	55 ± 7	0.014[b]	222 ± 11	ns
	Ad217NP	6	175 ± 5	ns	48 ± 12	ns	223 ± 12	0.035[b]
Exp. 2: rAd/plasmid prophylactic immunization	Untreated	17	168 ± 3		43 ± 8		212 ± 8	
	AdTA	9	170 ± 2	ns	54 ± 4	0.013[b]	227 ± 3.3	0.02[b]
	Ad168NP	8	171 ± 3	ns	61 ± 10	0.0009[b]	231 ± 11	0.0009[b]
Exp. 3: rAd/plasmid therapeutic immunization	Untreated	9	178 ± 1.5		60 ± 5		236 ± 6.6	
	AdTA	8	176 ± 2.2	ns	61 ± 7	ns	236 ± 8.3	ns
	Ad168NP	8	178 ± 1.5	ns	62 ± 6	ns	237 ± 10	ns

Analysis of Kaplan Meier survival curves.
[a] p: statistics using LogRank Test.
[b] Compared to untreated mice; ns: non-significant compared to untreated mice; Incubation phase: time from 139A inoculation to symptom onset; clinical phase: time from symptom onset to death.

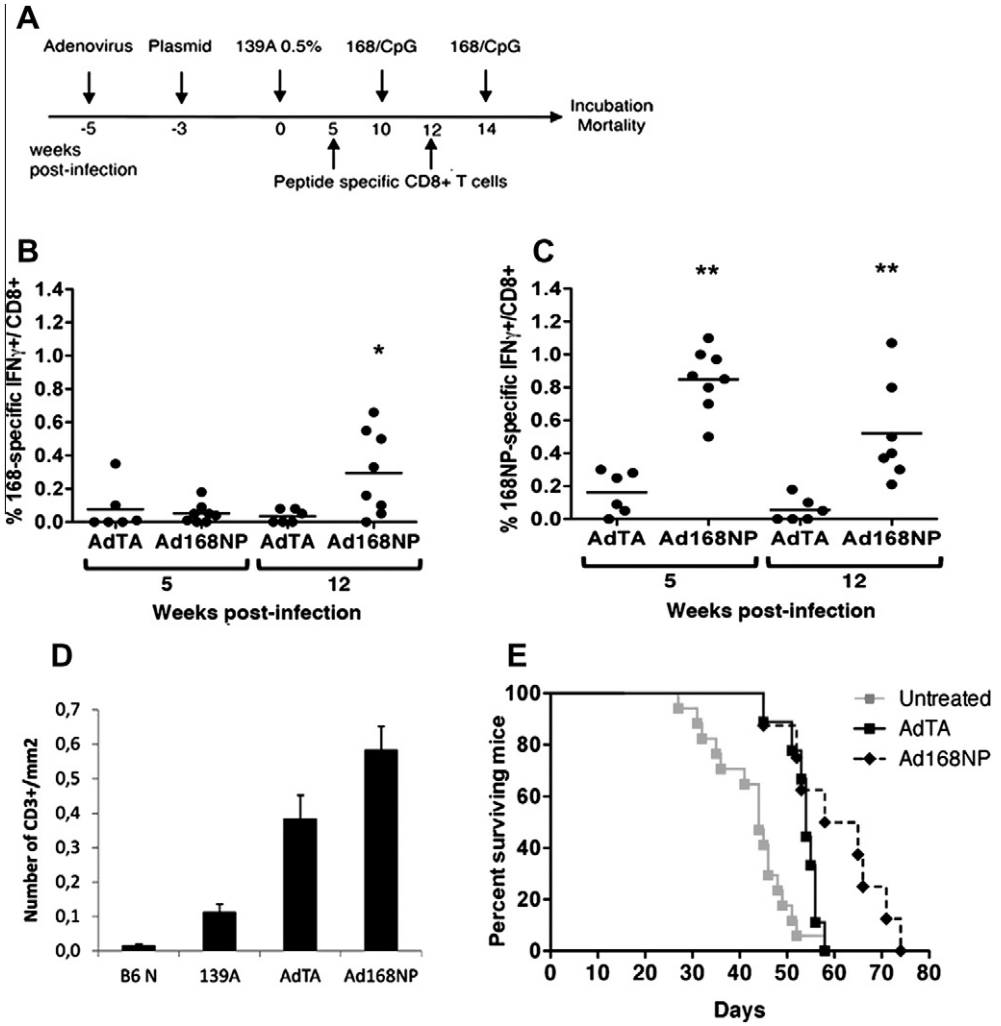

Fig. 6. Effect of additional peptide boosts to mice immunized with Ad168NP or control AdTA on specific $CD8^+$ T-cell responses and murine scrapie. (A) Time-sequence of immunization, plasmid/peptide boost and scrapie infection in C57Bl/6 mice. Wt mice were immunized with AdTA ($n = 9$) or Ad168NP/plasmids ($n = 8$) and inoculated 2 weeks later with 139A scrapie. They further received two additional injections of the native 168 peptide in CpG/IFA. Frequency in the blood of Ad168NP- or AdTA-immunized mice of $CD8^+$ T-cells producing intracellular IFN-γ after a 4 h activation with 168 (B) or 168NP (C) Significance: $^*p < 0.05$; $^{**}p < 0.01$. (D) Immunohistochemical analysis of T cells infiltrating the midbrain area at the terminal stage of 139A-infection in three mice per treatment. Paraffin brain sections were stained with anti-CD3mAb and revealed with an Alexa Fluor 488-conjugated goat anti-rabbit mAb. For each part of the brain, the total number of $CD3^+$ cells in three nonadjacent sections was determined and divided by the brain surface area in the section. The number of $CD3^+$ positive cells per mm^2 in AdTA- and Ad168NP-treated infected mice is shown comparatively to untreated infected and to normal C57BL/6 mice. Significance: $^*p < 0.05$; $^{**}p < 0.01$. (E) Mice were weekly examined for early signs of disease beginning at 5 months *pi* in each of the immunized groups. Mortality was recorded and Kaplan Meir survival curves was used to show the clinical stage duration which represents the time (days) elapsing from the beginning of the clinical symptoms to the death.

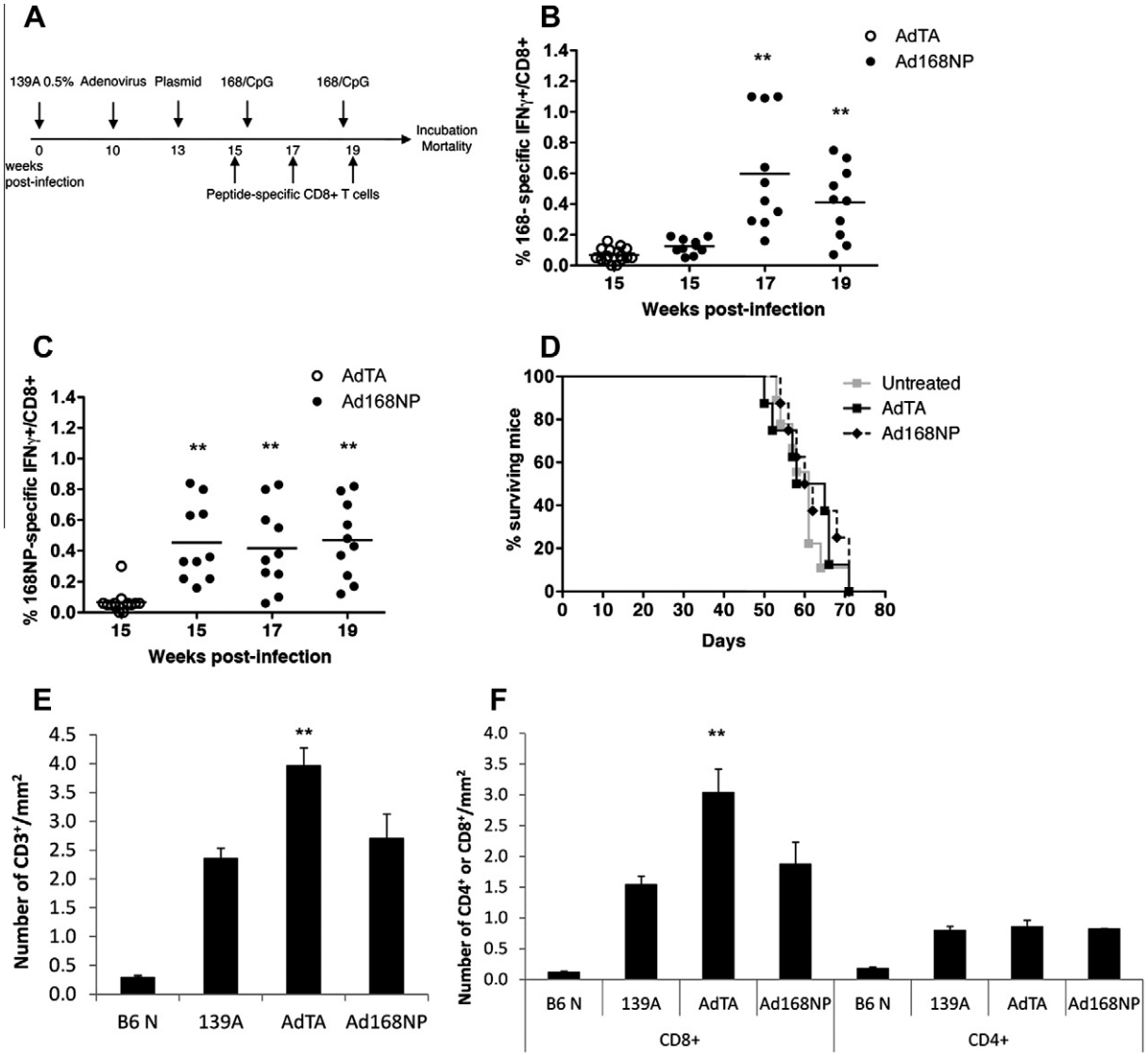

Fig. 7. Effect of therapeutic immunization with Ad168NP and 168 native peptide boosts on $CD8^+$-specific cell responses and murine scrapie. (A) Time-sequence of immunization, plasmid/peptide boost and scrapie infection in C57Bl/6 mice. Wt mice were first inoculated with 139A scrapie and immunized 10 weeks later with AdTA ($n = 10$) or Ad168NP ($n = 10$). They received two additional injections of the native 168 peptide in CpG/IFA. Frequency in the blood of Ad168NP- or AdTA-immunized mice of $CD8^+$ cells producing intracellular IFN-γ after brief activation with 168 (B) or 168NP (C) Significance: $^*p < 0.05$; $^{**}p < 0.01$. (D) Mice were weekly examined for early signs of disease beginning at 5 months *pi* in each of the immunized groups. Mortality was recorded and Kaplan Meir survival curves was used to show the clinical stage duration which represents the time (days) elapsing from the beginning of the clinical symptoms to the death. (E and F) Immunohistochemical analysis of T cells infiltrating the midbrain at the terminal stage of 139A infection. Frozen brain sections were stained with anti-CD3/CD4 or anti-CD3/CD8 mAbs and revealed with Alexa Fluor 488-conjugated goat anti-rabbit mAb and Alexa Fluor 594-conjugated goat anti-rat mAb. The number of positive cells per mm^2 was quantified as described above and compared to those in untreated infected mice and in normal C57BL/6 mice. Significance: $^{**}p < 0.01$.

responses specific for 168 were detectable only after the first native peptide injection ($0.60 \pm 0.11\%$; $n = 10$; $p < 0.0001$) and persisted after the second boost ($0.41 \pm 0.07\%$; $n = 10$; $p < 0.0001$; Fig. 7C). Importantly, the intensity of the response to the peptide 168 was similar or exceeded that of 168NP, indicating that injections of the native peptide elicited the expansion of specific $CD8^+$ T cells. However, *in vivo* lytic activity against 168NP-loaded CFSE-labeled targets was low in the two tested mice ($16 \pm 12\%$) (data not shown). In contrast to the results obtained when Ad immunization preceded 139A infection, vaccination in scrapie-incubating mice did not change the course of scrapie disease (Table 3; Exp. 3; Fig. 7D). Western Blot performed on the brains collected at 19 weeks pi indicated no difference in the amount of PrPSc between the groups (data not shown).

In this experiment, $CD3^+CD8^+$ and $CD3^+CD8^-$ T cell infiltration in the brain of terminally ill animals was quantified by immunofluorescence staining on frozen tissue sections. The number of $CD3^+/mm^2$ is higher than that measured in the previous experiment probably because of the partial antigenic retrieval in paraffin-embedded sections. However, the ratio of $CD3^+/mm^2$ between normal C57BL/6 and 139A-infected brain was identical (eight fold increase) when using the two different procedures. Compared to 139A-infected mice ($m = 2.35 \pm 0.18/mm^2$), $CD3^+$ cells further accumulated after immunization with AdTA ($m = 3.96 \pm 0.31/mm^2$; $p = 0.004$) but not with Ad168NP ($m = 2.70 \pm 0.43/mm^2$; ns) (Fig. 7E). Among infiltrating $CD3^+$ T cells in 139A-infected mice, $CD8^+$ significantly ($p = 0.019$) exceeded $CD4^+$ cells while in normal wt brain, the $CD4^+$ population was overrepresented (60%) indicating a $CD8^+$ cell migration in prion-infected mice (Fig. 7F). Following Ad treatments, the number of $CD8^+$ cells nearly doubled in AdTA-treated mice ($m = 3.04 \pm 0.38/mm^2$) as compared to untreated 139A-infected mice ($m = 1.54 \pm 0.14/mm^2$; $p = 0.0004$) but not in Ad168NP-treated mice

($m = 1.87 \pm 0.36/mm^2$; ns). The $CD4^+$ cell population increased four-fold in the brains of 139A-infected mice but remained unchanged under rAd treatments. In most cases, $CD8^+$ infiltrates were observed in the striatum and lateral and dorsal ventricles and, to a lesser extent, in the hypothalamus. Distribution of $CD4^+$ cells was patchy in the cerebral cortex, corpus callosum, and hypothalamus. No difference in the location of infiltrating T cells was observed between the AdTA and Ad168NP groups.

4. Discussion

These studies examined the possible influence of $CD8^+$ CTLs stimulated following PrP^c vaccination and the possible consequences in prion-inoculated mice. Our results suggest that *in vivo* stimulation of autoreactive $CD8^+$ CTLs specific for a natural PrP epitope triggers a protective rather than a detrimental effect on prion disease. The significant increase in the survival time of scrapie mice is attributable to an extension of the symptomatic phase and is associated with T cell infiltration in the parenchyma suggesting that PrP-specific $CD8^+$ T cells locally act with prions into the CNS.

Immunization of $Prnp^{-/-}$ mice with a plasmid containing the cDNA sequence of mPrP failed to raise CTLs against PrP while it efficiently elicited PrP-specific antibodies and $CD4^+$ T cells (Gregoire et al., 2004). Since immune tolerance could not be incriminated, we adopted another strategy to recruit a specific $CD8^+$ CTL repertoire without raising antibodies/$CD4^+$ cells against mPrP. $CD8^+$ T cells recognize short peptides anchored in the peptide groove of MHC class I molecules. The binding capacity of a given peptide and thus its immunogenicity are determined by the type of anchoring positions, which themselves depend on the presenting MHC molecule (Van der Burg et al., 1996). To identify epitopes potentially targeted by $CD8^+$ T cells, five candidate PrP nonamer peptides were selected using prediction algorithms and found to bind H-$2D^b$ with low affinity. When injected in combination with a $CD4^+$ helper PrP-unrelated epitope and CpG, none of the peptides elicited a specific IFNγ response in PrP-expressing wt mice as well as in $Prnp^{-/-}$ mice incriminating the low binding affinity and stability of the peptides rather than tolerance in the unresponsiveness. Nevertheless, we selected these low affinity epitopes because their CTL repertoire would likely escape thymic deletion in wt mice (Gross et al., 2004) and optimized the binding affinity of the PrP peptides. Indeed, substitutions at main anchor residues without affecting TCR contact residues constitute a common procedure to improve binding capacity and immunogenicity of antigenic peptides (Tourdot et al., 1997). Indeed, AA substitutions at anchor positions increased the binding affinity for H-$2D^b$ molecule for four of five modified peptides (NP-peptides). Vaccination with the NP-peptides induced significant frequencies of IFNγ-secreting T cells in response to the immunizing NP-peptides which were nevertheless lower in response to their native counterparts. Actually, predicting epitopes on the sole basis of their binding motif has a success rate of approximately 30% to reveal naturally processed peptides (Yewdell and Bennink, 1999). In this work, only 168 and 192 peptides were naturally processed and presented to the immune system by 1C11 cells, a neuronal cell line (Buc-Caron et al., 1990; Mouillet-Richard et al., 2000). Among the five tested NP-peptides, 168NP, 192NP and 217NP but not 103NP and 166NP induced T cells that were lytic *in vivo* for NP- but not native peptide-loaded target cells. Only CTLs specific for 217NP were cytotoxic *in vitro* for NP and native peptide-loaded targets but not for 1C11 cells likely related to 217 peptide processing deficit. The lytic capacity of anti-217NP $CD8^+$ T cells is potentially associated with their unique capacity to secrete TNFα (data not shown). Altogether, these data indicate that the $CD8^+$ T cell repertoire specific for low-affinity PrP-derived epitopes are peripherally present in wt mice but requires strong immunizing procedures to be stimulated.

Immunization with any of the three NP-peptides mixed with I-A^b epitope/CpG/IFA of wt mice that were later infected with 139A-scrapie strain elicited peptide-specific IFNγ secreting $CD8^+$ T cells. However, these responses failed to delay disease progression. Specific immune responses enhancement was achieved by introducing minigenes encoding $CD8^+$ epitopes into Ad vectors which bring strong helper signals (Tatsis and Ertl, 2004). Minigenes were reported to be more efficient than full-length protein constructs for eliciting CTL responses (Tine et al., 2005), likely because proteasomal processing is not required before association with MHC class I molecules, thus optimizing antigen delivery (Leifert et al., 2004). 168NP was selected for minigenes construction based on its capacity stimulates a $CD8^+$ cytolytic repertoire which recognized a natural peptide nearly as well as the NP-modified one. 217NP stimulates a large $CD8^+$ cytolytic repertoire which recognized the NP-modified peptide but not a PrP-expressing cell. Prophylactic immunization with Ad168NP did not delay symptom onset but, unexpectedly, significantly extended the scrapie-associated symptomatic phase. Additional boosts with 168 amplified the $CD8^+$ T cell pool specific for the 168 native peptide and further prolonged clinical phase. The partial positive effect obtained with AdTA can be viewed as a classical adjuvant effect associated with non-specific immune stimulation and significant therapeutic benefits, as reported in two earlier studies (Tal et al., 2003; Pilon et al., 2007). However, the lack of protection following Ad217NP immunization, likely originating from peptide processing deficit, suggest that the prolongation of the clinical phase can be in part attributed to a peptide-related specific effect. Our data favor a role for PrP-specific $CD8^+$ T cells in this effect, since, in this model anti-PrP $CD4^+$ T cells and/or antibodies can be excluded. The same Ad168NP immunization procedure performed with 139A-incubating mice is not associated with an extended clinical phase. We showed previously that $PrP_{158\text{-}197}$-specific $CD4^+$ T cell responses were blunted when immunization was performed in 139A-incubating mice (Sacquin et al., 2008). *In vivo* and *in vitro* depletion of $CD4^+CD25^+$ T cells completely restores the *in vitro* T-cell response to $PrP_{158\text{-}197}$, suggesting the development of an immune regulatory mechanism during prion accumulation.

Many vaccination regimens in experimental mouse models of scrapie resulted in prolonged incubation periods, which were most often ascribed to anti-PrP antibodies (Pankiewicz et al., 2006; White et al., 2003; Peretz et al., 2001; Polymenidou et al., 2004; Bachy et al., 2010; Rosset et al., 2009). To our knowledge, our study constitutes the prime evidence that an immune manipulation can interfere with prion progression during the symptomatic period. We propose a role for peripherally-induced PrP-specific T cells since prolongation of the symptomatic phase correlates with $CD3^+$ T cell recruitment into the CNS. Within the few naïve $CD3^+$ T cells found in the normal CNS, the $CD4^+$ population was overrepresented (60%). However, a T cell recruitment that is dominated by $CD8^+$ cells (66%) is triggered by the accumulation of PrP^{Sc} in the brain of 139A-infected mice, confirming the earlier observations (Betmouni et al., 1996; Lewicki et al., 2003). In addition, as only activated T cells can enter the brain, peripheral $CD8^+$ cytolytic T cells stimulated by 168 might be able to migrate and to be entrap into the brain when locally activated by antigen encounter. $CD8^+$ T cells invading in the brains of AdTA-treated mice may be composed of bystander T cells activated by Ad antigens that migrate from the periphery, patrol into the CNS and recirculate in the absence of their specific antigens. Immunization with Ad168NP in scrapie-incubating mice induced IFNγ-secreting $CD8^+$ T cells that did not influence disease progression nor infiltrated the brain. In this assay, the number of $CD4^+$ cells remained constant in the brain of 139A-infected mice whatever the treatment. The absence of

in vivo lytic capacity of peripheral $CD8^+$ T cells specific for Ad168NP, suggests that cytotoxic function is important for the extension of the symptomatic phase associated to prion diseases.

Strikingly, the infiltration of the brain by self reactive $CD8^+$ T cells was not associated with CNS tissue damage. The weak MHC class I molecule expression on neurons (Joly and Oldstone, 1992) or/and their resistance to perforin-mediated lysis by CTLs (our observation and Medana et al., 2000), support the hypothesis that neurons are not the main target of anti-168 $CD8^+$ T cells. Another possibility is that these $CD8^+$ T cells might eliminate PrP-presenting cells such as microglial cells or astrocytes, which are recruited and activated in the vicinity of PrP^{Sc} aggregates and expressed high level of class I molecules (Marella and Chabry, 2004; Eikelenboom et al., 2002). Moreover, astrocytes are involved as neurons in the PrP^c to PrP^{Sc} conversion. Beyond the capacity of CTLs to damage CNS cells (Mars et al., 2011), $CD8^+$ T cells might exert regulatory functions (Chess and Jiang, 2004; Zozuyla and Wiendl, 2008; Mars et al., 2011).Treatment of MS patients with glatiramer acetate, a synthetic copolymer of four AAs, increases the capacity of $CD8^+$ T cells to kill $CD4^+$ T cells of any specificity in a MHC-I-dependent manner (Tennakoon et al., 2006) or myelin-specific $CD4^+$ T cells in a HLA-E-restricted manner (Correale and Villa, 2008). Further experiments will be required to decipher the mechanism and the exact target underlying $CD8^+$ T-cell actions.

To conclude, *in vivo* stimulation of a CTL repertoire specific for a natural PrP-derived epitope triggers a time extension of prion disease-associated symptomatic phase, which correlates with T-cell infiltration into the CNS. However, the development of a safe vaccine for prion diseases requires the understanding of the mechanism underlying the effect of PrP-specific $CD8^+$ T cells.

Acknowledgments

This work was supported by funds from the INSERM and the Neuroprion network of excellence, European FP6 program. Antoine Sacquin received a Ph.D. fellowship from the nonprofit France Alzheimer Association.

Appendix A. Supplementary data

Supplementary data associated with this article can be found, in the online version, at http://dx.doi.org/10.1016/j.bbi.2012.04.002.

References

Bachy, V., Ballerini, C., Gourdain, P., Prignon, A., Iken, S., et al., 2010. Mouse vaccination with dendritic cells loaded with prion protein peptides overcomes tolerance and delays scrapie. J. Gen. Virol. 91, 809–820.

Beers, D., Zhao, W., Liao, B., Kano, O., Wang, J., Appel, S., Henkel, J.S., 2011. Neuroinflammation modulates distinct regional and temporal clinical responses in ALS mice. Brain Behav. Immun. 25 (5), 1025–1035.

Bendheim, P.E., Brown, H.R., Rudelli, R.D., Scala, L.J., Goller, N.L., et al., 1992. Nearly ubiquitous tissue distribution of the scrapie agent precursor protein. Neurology 42, 149–156.

Beringue, V., Vilette, D., Mallinson, G., Archer, F., Kaisar, M., et al., 2004. PrPSc binding antibodies are potent inhibitors of prion replication in cell lines. J. Biol. Chem. 279, 39671–39676.

Betmouni, S., Perry, V.H., Gordon, J.L., 1996. Evidence for an early inflammatory response in the central nervous system of mice with scrapie. Neuroscience 74, 1–5.

Branger, C., Sonrier, C., Chatrenet, B., Klonjkowski, B., Ruvoen-Clouet, N., Aubert, A., André-Fontaine, G., Eloit, M., 2001. Identification of the hemolysis-associated protein 1 as a cross-protective immunogen of Leptospira interrogans by adenovirus-mediated vaccination. Infect. Immun. 69, 6831–6854.

Brochard, V., Combadiere, B., Prigen, A., Laouar, Y., Perrin, A., Beray-Berthat, V., Bonduelle, O., et al., 2009. Infiltration of CD4+ lymphocytes into the brain contributes to neurodegeneration in a mouse model of Parkinson disease. J. Clin. Invest. 119, 182–192.

Buc-Caron, M.H., Launay, J.M., Lamblin, D., Kellermann, O., 1990. Serotonin uptake, storage, and synthesis in an immortalized committed cell line derived from mouse teratocarcinoma. Proc. Natl. Acad. Sci. USA 87, 1922–1926.

Chess, L., Jiang, H., 2004. Resurrecting CD8+ suppressor T cells. Nat. Immunol. 5, 469–471.

Correale, J., Villa, A., 2008. Isolation and characterization of CD8+ regulatory T cells in multiple sclerosis. J. Neuroimmunol. 195, 121–124.

Eikelenboom, P., Bate, C., Van Gool, W.A., Hoozemans, J.J.M., Rozemuller, J.M., Veerhuis, R., et al., 2002. Neuroinflammation in Alzheimer's disease and prion disease. Glia. 40, 232–239.

Ethell, D.W., Shippy, D., Cao, C., Cracchiolo, J.R., Runfeld, M., Blake, B., 2006. Aβ-specific T-cells reverse cognitive decline and synaptic loss in Azheimer's mice. Neurobiol. Disease 23, 351–361.

Ferrer, I., Boada Rovira, M., Sanchez Guerra, M.L., Rey, M.J., Costa-Jussa, F., 2004. Neuropathology and pathogenesis of encephalitis following amyloid-β immunization in Alzheimer's disease. Brain Pathol. 14 (1), 11–20.

Fernandez-Borges, N., Brun, A., Whitton, J.L., Parra, B., Diaz-San Segundo, F., 2006. DNA vaccination can break immunological tolerance to PrP in wild-type mice and attenuates prion disease after intracerebral challenge. J. Virol. 80, 9970–9976.

Gilman, S., Koller, M., Black, R.S., Jenkins, L., Griffith, S.G., Fox, N.C., et al., 2005. Clinical effects of Aβ immunization (AN1792) in patients with AD in an interrupted trial. Neurology 64, 1553–1562.

Gourdain, P., Gregoire, S., Iken, S., Bachy, V., Dorban, G., et al., 2009. Adoptive transfer of T lymphocytes sensitized against the prion protein attenuates prion invasion in scrapie-infected mice. J. Immunol. 183, 6619–6628.

Gregoire, S., Logre, C., Metharom, P., Loing, E., Chomilier, J., et al., 2004. Identification of two immunogenic domains of the prion protein–PrP–which activate class II-restricted T cells and elicit antibody responses against the native molecule. J. Leukoc. Biol. 76, 125–134.

Gross, D.A., Graff-Dubois, S., Opolon, P., Cornet, S., Alves, P., Bennaceur-Gricelli, A., Faure, O., et al., 2004. High vaccination efficiency of low-affinity epitopes in anti-tumor immunotherapy. J. Clin. Invest. 113 (3), 425–433.

Iken, S., Bachy, V., Gourdain, P., Lim, A., Gregoire, S., Chaigneau, T., Aucouturier, P., Carnaud, C., 2011. Th2-polarized PrP-specific transgenic T-cells confer partial protection against murine scapie. Plos Path. 7, e1002216.

Isaacs, J.D., Ingram, R.J., Collinge, J., Altmann, D.M., Jackson, G.S., 2006. The human prion protein residue 129 polymorphism lies within a cluster of epitopes for T cell recognition. J. Neuropathol. Exp. Neurol. 65, 1059–1068.

Joly, E., Oldstone, M.B., 1992. Neuronal cells are deficient in loading peptides onto MHC class I molecules. Neuron 8, 1185–1190.

Kaiser-Schulz, G., Heit, A., Quintanilla-Martinez, L., Hammerschmidt, F., Hess, S., et al., 2007. Polylactide-coglycolide microspheres co-encapsulating recombinant tandem prion protein with CpG-oligonucleotide break self-tolerance to prion protein in wild-type mice and induce CD4 and CD8 T cell responses. J. Immunol. 179, 2797–2807.

Lewicki, H., Tishon, A., Homann, D., Mazarguil, H., Laval, F., et al., 2003. T cells infiltrate the brain in murine and human transmissible spongiform encephalopathies. J. Virol. 77, 3799–3808.

Levavasseur, E., Metharom, P., Dorban, G., Nakano, H., Kakiuchi, T., et al., 2007. Experimental scrapie in 'plt' mice. an assessment of the role of dendritic-cell migration in the pathogenesis of prion diseases. J. Gen. Virol. 88, 2353–2360.

Leifert, J.A., Rodriguez-Carreno, M.P., Rodriguez, F., Whitton, J.L., 2004. Targeting plasmid-encoded proteins to the antigen presentation pathways. Immunol. Rev. 199, 40–53.

Ma, J., Lindquist, S., 2002. Conversion of PrP to a self-perpetuating PrPSc-like conformation in the cytosol. Science 298, 1785–1788.

Marella, M., Chabry, J., 2004. Neurons and astrocytes respond to prion infection by inducing microglia recruitment. J. Neurosci. 24 (3), 620–627.

Mars, L.T., Saikali, P., Liblau, R.S., Arbour, N., 2011. Contribution of CD8 T lymphocytes to the immunopathogenesis of multiple sclerosis and its animal models. Biochem. Biophy. Acta 1812, 151–161.

Mars, L.T., Bauer, J., Gross, D.A., Bucciarelli, F., Firat, H., Hudrisier, D., Lemonnier, F., Kosmatopoulos, K., Liblau, R., 2007. CD8 T cell responses to myelin oligodendrocyte glycoprotein-derived peptides in humanized HLA-A0201-transgenic mice. J. Immunol. 179, 5090–5098.

Mc Farland, H.F., Martin, R., 2007. Multiple sclerosis: a complicated picture of autoimmunity. Nat. Immunol. 8, 913–919.

Medana, I.M. et al., 2000. MHC class I-restricted killing of neurons by virus-specific CD8+ T lymphocytes is effected through the Fas/FasL, but not perforin pathway. Eur. J. Immunol. 30, 3623–3633.

Mouillet-Richard, S., Mutel, V., Loric, S., Tournois, C., Launay, J.M., Kellermann, O., 2000. Regulation by neurotransmitter receptors of serotonergic or catecholaminergic neuronal cell differentiation, J. Biol. Chem. 275, 9186–9192.

Neumann, H., Medana, I.M., Bauer, J., Lassmann, H., 2002. Cytotoxic T lymphocytes in autoimmune and degenerative CNS disease. Trends in Neurosci. 25, 313–319.

Pankiewicz, J., Prelli, F., Sy, M.S., Kascsak, R.J., Kascsak, R.B., et al., 2006. Clearance and prevention of prion infection in cell culture by anti-PrP antibodies. Eur. J. Neurosci. 23, 2635–2647.

Peretz, D., Williamson, R.A., Kaneko, K., Vergara, J., Leclerc, E., et al., 2001. Antibodies inhibit prion propagation and clear cell cultures of prion infectivity. Nature 412, 739–743.

Pilon, J., Loiacono, C., Okeson, D., Lund, S., Vercauteren, K., et al., 2007. Anti-prion activity generated by a novel vaccine formulation. Neurosci. Lett. 429, 161–164.

Polymenidou, M., Heppner, F.L., Pellicioli, E.C., Urich, E., Miele, G., et al., 2004. Humoral immune response to native eukaryotic prion protein correlates with anti-prion protection. Proc. Natl. Acad. Sci. USA 101, 14670–14676.

Prusiner, S.B., Scott, M.R., DeArmond, S.J., Cohen, F.E., 1998. Prion protein biology. Cell 93, 337–348.

Rosset, M.B., Ballerini, C., Gregoire, S., Metharom, P., Carnaud, C., et al., 2004. Breaking immune tolerance to the prion protein using prion protein peptides plus oligodeoxynucleotide-CpG in mice. J. Immunol. 172, 5168–5174.

Rosset, M.B., Sacquin, A., Lecollinet, S., Chaigneau, T., Adam, M., et al., 2009. Dendritic cell-mediated-immunization with xenogenic PrP and adenoviral vectors breaks tolerance and prolongs mice survival against experimental scrapie. PLoS ONE 4, e4917.

Sacquin, A., Bergot, A.S., Aucouturier, P., Bruley-Rosset, M., 2008. Contribution of antibody and T cell-specific responses to the progression of 139A-scrapie in C57BL/6 mice immunized with prion protein peptides. J. Immunol. 181, 768–775.

Schenk, D., Barbour, R., Dunn, W., Gordon, G., Grajeda, H., Guido, T., et al., 1999. Immunization with amyloid-β attenuates Alzheimer-disease-like pathology in the PDAPP mouse. Nature 400, 173–177.

Souan, L., Tal, Y., Felling, Y., Cohen, I.R., Taraboulos, A., et al., 2001. Modulation of proteinase-K resistant prion protein by prion peptide immunization. Eur. J. Immunol. 31, 2338–2346.

Tal, Y., Souan, L., Cohen, I.R., Meiner, Z., Taraboulos, A., et al., 2003. Complete Freund's adjuvant immunization prolongs survival in experimental prion disease in mice. J. Neurosci. Res. 71, 286–290.

Tatsis, N., Ertl, H.C., 2004. Adenoviruses as vaccine vectors. Mol. Ther. 10, 616–629.

Tennakoon, D.K., Mehta, R.S., Ortega, S.B., Tennakoon, M.K., Racke, R.J., Karandikar, N.J., 2006. Therapeutic induction of regulatory, cytotoxic CD8+ T cells in Multiple Sclerosis. J. Immunol. 176, 7119–7129.

Tine, J.A., Firat, H., Payne, A., Russo, G., Davis, S.W., et al., 2005. Enhanced multiepitope-based vaccines elicit CD8+ cytotoxic T cells against both immunodominant and cryptic epitopes. Vaccine 23, 1085–1091.

Tourdot, S., Oukka, M., Manuguerra, J.C., Magafa, V., Vergnon, I., et al., 1997. Chimeric peptides: a new approach to enhancing the immunogenicity of peptides with low MHC class I affinity: application in antiviral vaccination. J. Immunol. 159, 2391–2398.

Van der Burg, S.H., Visseren, M.J.W., Brandt, R.M.P., Kast, W.M., Melief, C.J.M., 1996. Immunogenicity of peptides bound to MHC class I molecules depends on the MHC-peptide complex stability. J. Immunol. 156, 3308–3314.

White, A.R., Enever, P., Tayebi, M., Mushens, R., Linehan, J., et al., 2003. Monoclonal antibodies inhibit prion replication and delay the development of prion disease. Nature 422, 80–83.

Yewdell, J.W., Bennink, J.R., 1999. Immunodominance in major histocompatibility complex class I-restricted T lymphocyte responses. Annu. Rev. Immunol. 17, 51–88.

Zozuyla, A.L., Wiendl, H., 2008. The role of CD8 suppressors versus destructors in autoimmune central nervous system inflammation. Hum. Immunol. 69 (11), 797–804.